Structure-Based Design of Hepatitis C Virus Vaccines that Elicit Neutralizing Antibody Responses to a Conserved Epitope

Brian G. Pierce[1,2#], Elisabeth N. Boucher[3], Kurt H. Piepenbrink[4*], Monir Ejemel[3], Chelsea A. Rapp[4], William D. Thomas Jr[3], Eric J. Sundberg[4,5], Zhiping Weng[1] and Yang Wang[3#]

[1]Program in Bioinformatics and Integrative Biology, University of Massachusetts Medical School, Worcester, MA 01655, USA

[2]University of Maryland Institute for Bioscience and Biotechnology Research, Rockville, MD 20850, USA

[3]MassBiologics, University of Massachusetts Medical School, Boston, MA 02126, USA

[4]Institute of Human Virology, University of Maryland School of Medicine, Baltimore, MD 21201, USA

[5]Departments of Medicine and of Microbiology & Immunology, University of Maryland School of Medicine, Baltimore, MD 21201, USA

*Present address: Department of Food Science and Technology, University of Nebraska-Lincoln, Lincoln, NE 68588, USA

Running Title: Structure-Based Design of HCV Vaccines

#Address correspondence to Brian G. Pierce (pierce@umd.edu) or Yang Wang (yang.wang@umassmed.edu).

ABSTRACT

Despite recent advances in therapeutic options, hepatitis C virus (HCV) remains a severe global disease burden, and a vaccine can substantially reduce its incidence. Due to its extremely high sequence variability, HCV can readily escape the immune response, thus an effective vaccine must target conserved, functionally important epitopes. Using the structure of a broadly neutralizing antibody in complex with a conserved linear epitope from the HCV E2 envelope glycoprotein (residues 412-423; epitope I), we performed structure-based design of immunogens to induce antibody responses to this epitope. This resulted in epitope-based immunogens based on a cyclic defensin protein, as well as a bivalent immunogen with two copies of the epitope on the E2 surface. We solved the x-ray structure of a cyclic immunogen in complex with the HCV1 antibody and confirmed preservation of the epitope conformation and the HCV1 interface. Mice vaccinated with our designed immunogens produced robust antibody responses to epitope I, and their serum could neutralize HCV. Notably, the cyclic designs induced greater epitope-specific responses and neutralization than the native peptide epitope. Beyond successfully designing several novel HCV immunogens, this study demonstrates the principle that neutralizing anti-HCV antibodies can be induced by epitope-based, engineered vaccines and provides the basis for further efforts in structure-based design of HCV vaccines.

46 **IMPORTANCE**
47

48 Hepatitis C virus is a leading cause of liver disease and liver cancer, with approximately 3% of
49 the world's population infected. To combat this virus, an effective vaccine would have distinct
50 advantages over current therapeutic options, yet experimental vaccines have not been successful
51 to date, due in part to the virus's high sequence variability leading to immune escape. In this
52 study we rationally designed several vaccine immunogens based on the structure of a conserved
53 epitope that is the target of broadly neutralizing antibodies. In vivo results in mice indicated that
54 these antigens elicited epitope-specific neutralizing antibodies, with varying degrees of potency
55 and breadth. These promising results suggest that a rational design approach can be used to
56 generate an effective vaccine for this virus.

57

58
59

INTRODUCTION

Hepatitis C virus (HCV) is a major global health concern, infecting 3% of the world's population (1). The majority of those infected progress to chronic HCV infection, which often leads to cirrhosis, liver failure, and hepatocellular carcinoma, a deadly liver cancer (2). Liver transplantation, undertaken for those with cirrhosis and liver cancer, does not eliminate the virus completely, resulting in viral rebound and infection of the transplanted liver (2). Despite advances in treatment methods for HCV, including recently approved direct acting antivirals, high treatment cost and a high rate of asymptomatic and untreated infections make a prophylactic vaccine necessary for global control of HCV (1).

After decades of research, as well as several candidates in Phase I and Phase II clinical trials (3), no approved HCV vaccine is available. This is in part due to the high diversity of the virus within individuals, arising from error-prone replication and estimated to be 10-fold greater than HIV, leading to generation of a number of viral quasispecies that allow it to readily escape from the immune response (4). The identification of broadly neutralizing antibodies (bnAbs) that target conserved and functionally important regions of the E1 and E2 glycoproteins on the viral surface (5), as well as structural characterization of several bnAb-epitope complexes (6-13), provide a major opportunity to design vaccines that induce robust antibody responses to one or more of these epitopes (14). Such structure-based vaccine design approaches have been explored for other viruses such as HIV (15, 16), influenza (17, 18), and RSV (19, 20), with promising results, though in some cases neutralizing antibodies were not successfully induced in vivo, possibly due to the epitope's context on the viral surface (15) or immunological variability

among animal models (20). In the context of HCV, one candidate for immunogen design is the epitope bound by the bnAb HCV1 (21).

HCV1 was generated by immunization of humanized mice with soluble E2 (21), and targets a continuous epitope on the surface of E2 (residues 412-423, referred to as epitope I), which is also recognized by a variety of human (22) and murine (23, 24) mAbs. Tests of the HCV1 mAb in chimpanzees showed evidence of protection from HCV infection as well as reduction in viral load (25), and in humans HCV1 treatment resulted in significant delay in viral rebound, versus placebo, following liver transplantation (26). Structural characterization of the HCV1 mAb in complex with this epitope found that epitope I adopts a β hairpin conformation with a type I' β turn (6), which was later observed in the structures of mAb AP33 (8) and two other mAbs (9) bound to epitope I. Epitope I is targeted by neutralizing antibodies that block E2 binding to the human CD81 receptor which is required for cell entry, and is distinguished from other CD81-associated sites on E2 as it is a continuous rather than conformational epitope (27); this is supported by a recent global E2 alanine scanning study that assessed binding determinants using a panel of 16 E2-targeting mAbs (28). Due to this apparent decoupling and lack of dependency on the remainder of E2, epitope I is of particular interest for structure-based immunogen design efforts, as noted by others (14).

Given the low seroreactivity to this epitope in infected humans (< 2.5% out of 245 patient samples) (29), the lack of initial reported success inducing antibodies in mice using the linear epitope (21), and its observed flexibility which has been highlighted in several recent structural studies (12, 30), we performed rational engineering to stably present this antibody-bound

structure to the immune system and improve the antibody response to this conserved epitope. We also designed a novel protein using the E2 core protein structure (7), generating a bivalent E2 core antigen presenting two copies of epitope I on its surface. After confirming antibody binding of designs, as well and atomic level structure of a cyclic design, and in vivo immunogenicity of these designs, to compare their effectiveness at eliciting antibodies that bind epitope I, and tested sera of immunized mice for HCV neutralization of several HCV genotypes.

MATERIALS AND METHODS

Scaffold selection. A set of 7626 potential scaffold structures was downloaded from the Protein Data Bank (PDB) (31) in February, 2013. All structures were monomeric (one protein chain in the biological assembly), expressed in E. coli, determined by x-ray crystallography, and contained fewer than 200 residues. The structural alignment program FAST (32) was used to identify any structurally similar region to epitope I (PDB code 4DGY, chain A) within each structure. Approximately half of the structures (4200) contained regions identified by FAST as structurally similar to the epitope; these results were analyzed to determine length of match, root-mean-square distance (RMSD) to the epitope (both computed by FAST), and accessibility for antibody binding. The latter value was determined by counting the number of atomic contacts (< 4.0 Å) between the HCV1 mAb and scaffold (excluding the epitope-matching residues), after superposing the scaffold onto the epitope in the HCV1-epitope complex structure using FAST.

Protein expression and purification. The nucleic acid sequences encoding HCV E2 (genotype 1a isolate H77, Genbank accession number NC004102) aa 384-661 (referred to as $E2_{661}$) and its designed truncated constructs (T1, T2, T3) were synthesized and cloned into a mammalian

128 expression vector, pcDNA3.1 (Life Technologies) in frame with an N-terminal histidine (His)
129 tag. Cloned vectors were transfected into HEK-293T cells using Lipofectamine 2000 (Life
130 Technologies) as described by the manufacturer. Cells were grown to confluence in T150 in 15
131 ml of DMEM with 10% of FBS. Thirty micrograms of DNA were mixed with 75 µl of
132 Lipofectamine 2000 and the mixture was added to the cells for overnight incubation at 37 °C.
133 Medium was removed 24 hours post-transfection and replaced with fresh complete DMEM. 3
134 mM sodium butyrate (Sigma-Aldrich) was added to the media 48 hours post transfection and the
135 supernatants were harvested after additional 24-hour incubation. Filtered supernatant were mixed
136 with Ni-NTA agarose (Life Technologies) for 2 hours at room temperature and proteins were
137 eluted with 250 mM imidazole (Sigma-Aldrich). Eluted proteins were dialyzed against PBS,
138 concentrated and stored in single use aliquots at -80°C. Protein integrity and purity were
139 evaluated by Coomassie stained SDS-PAGE and Western blot using mouse anti-His antibody.
140
141 **Peptides.** Linear and cyclized peptides including the H77 epitope I sequence
142 (QNIQLINTNGSWHINSTK, CQLINTNGSWHINCK) were produced at New England Peptide
143 (Gardner, MA), conjugated to bovine serum albumin (BSA) or keyhole limpet hemocyanin
144 (KLH) carrier protein via gluteraldehyde at the C-terminal lysine side chain. For peptides
145 without backbone cyclization, N-termini were modified via acetylation to improve coupling and
146 prevent N-terminal glutamine conversion to pyroglutamic acid (in the case of linear peptide).
147 Peptides produced for immunogenicity studies were N-glycosylated at the position
148 corresponding to N417 with the N-acetylglucosamine (GlcNAc) glycan.
149

ELISA. 96-well plates were coated with antigens (peptide, $E2_{661}$, or E2 truncations), at a concentration of 2 μg/ml, followed by incubation overnight at 4°C. Mouse serum or purified antibody was added to the 96-well plates and incubated for 1 hour at room temperature. Antibody binding was detected with anti-human alkaline phosphatase secondary antibody and PNPP substrate.

Surface plasmon resonance. All SPR experiments were performed using a Biacore T100 instrument (GE Healthcare). Soluble BSA (NE Biolabs), C2 peptide-BSA, C1 peptide-BSA, and the linear peptide-BSA in 10 mM sodium acetate, pH 4.0 were immobilized on a CM5 sensor chip via standard amine coupling procedure at a density of 1322 RU to flow cell 1, 796 RU to flow cell 2, 124 RU to flow cell 3 and 101 RU to flow cell 4, respectively. HBS-X buffer (10 mM HEPES, 150 mM NaCl, 0.05% Tween) was used as a running buffer. BSA coupled to the sensor chip in flow cell 1 was used as the negative control surface. A concentration series of HCV1 mAb (125-1.9 nM) in running buffer was injected over flow cells 1-4 for 60 s per injection and allowed to dissociate for 300 s. Between binding cycles, the sensor chip surface was regenerated by washing with 2 M NaCl. Kinetic paramenters and affinity constants for all interactions were calculated using a kinetic model for bivalent analytes (as HCV1 was in IgG rather than Fab format) with the Biacore T100 evaluation software 2.0.4.

X-ray crystallography. HCV1 Fab was separated from the Fc by papain using standard protocols, purified by size exclusion chromatography on a GE Superdex S200, concentrated to 10 mg/ml in 20 mM Tris, 100 mM NaCl pH 8.3 and incubated with a tenfold excess of the C1 peptide (CQLINTNGSWHINCK). Crystals formed after one week by vapor diffusion in 0.2 M

calcium acetate, 0.1 M MES pH 6.0, 20% PEG 4000 at a drop ratio of 1:1. Glycerol was added at 20% as a cryo-protectant and data was collected at the Stanford Synchrotron Radiation Lightsource, beamline 9-2 and the Advanced Photon Source, beamline 23-ID-D. The data were integrated by XDS at 2.26 Å resolution, phased using molecular replacement by Phaser, built using Coot, and refined by Phenix refine and Refmac (33-36), and deposited in the PDB under accession code 5KZP.

Modeling HCV1 mAb bound to E2. Modeling the HCV1 mAb bound to E2 at residues 412-423 was performed by aligning the HCV1-epitope I complex (PDB code 4DGY) onto the E2 core structure (PDB code 4MWF, chain D) using root-mean-square fitting of the backbone atoms of shared E2 residue N423. The FloppyTail algorithm in Rosetta (37) was then used to perform minimization of HCV1-epitope I in the context of E2 core, to reduce clash between HCV1 and E2 core, treating the backbone of residue 423 as a flexible hinge. 100 models were generated, of which the top model was selected based on Rosetta score and paucity of mAb contacts with E2 core (as HCV1 targets a linear epitope, extensive contacts with E2 core are not likely, as supported by a global alanine scanning study with other antibodies targeting epitope I (28)). HCV1 was fit by backbone superposition of epitope I residues onto residues 629-640 of E2 core to model its engagement of the transplanted epitope.

In vivo studies. CD-1 mice (Charles River) were injected intraperitoneally with purified protein mixed with Sigma Adjuvant System (SAS) adjuvant (Sigma Aldrich) with 50 µg prime and four 10 µg boosts given weekly, except for a gap of two to three weeks between second and third

boost. Animals were sacrificed approximately 10 days after final injection, and sera were collected for neutralization and binding assays.

HCV transfection, infection and neutralization assays. Pseudovirus was generated by using a replication defective HIV backbone containing a firefly luciferase gene to direct luciferase expression in target cells (pNL4-3.Luc.R–E–, obtained through the AIDS Research and Reference Program, Division of AIDS, NIAID, NIH from Dr. Nathaniel Landau). The nucleic acid sequences encoding HCV E1E2 glycoprotein from isolates H77 (genotype 1a), 1b-#2 (genotype 1b), and 4a-MJ (genotype 4a), GenBank accession numbers NC004102, GQ259488, GQ379230, respectively, were cloned into pcDNA3.1 vector as described previously (21). The pcDNA-E1E2 vectors were co-transfected with pNL4-3.Luc.R-E- into 293T cells using Lipofectamine2000 (Life Technologies). Pseudoviral particles were harvested 48-72 h post transfection, concentrated using a Centricon 70 concentrator (Millipore), aliquoted and stored frozen at 80°C. Before assessing antibody neutralization, a titration of HCVpp was performed on Hep3B cells to determine what volume of virus generated 50,000 cps in the infection assay. The appropriate volume of HCVpp was pre-incubated with varying dilutions of mouse serum or HCV1 for 1 h at room temperature before adding to Hep3B cells. After incubation for 72 h (38), infection was quantified by luciferase detection (Bright-Glo reagent, Promega) and read in a Victor 3 plate reader (Perkin Elmer) for light production.

Figures. Figures of molecular structures were generated using PyMOL (Schrodinger, LLC), and plots of ELISA and neutralization data were generated using GraphPad Prism.

RESULTS

Scaffold search and design of cyclic antigens. As noted previously (38), epitope I is highly conserved across HCV genotypes (Fig. 1A), and key binding residues for HCV1 (6) are nearly fully conserved (L413: 99.8%, N415: 96.6%, G418: 99.8%, W420: 99.8% in over 600 E2 sequences downloaded from the LANL HCV database (39)). To identify proteins to present the epitope I structure in its β hairpin conformation and type I' β turn, we searched a set of approximately 7600 crystal structures of monomeric proteins downloaded from the Protein Data Bank (31) using the FAST structural alignment algorithm (32) for substructures matching epitope I in the HCV1 mAb-epitope I crystal structure (6). All structures including matches identified by FAST (approximately half of the original structures) were screened for match length, backbone RMSD to the epitope, protein size, and antibody accessibility. To avoid potentially immunogenic regions in scaffolds that would reduce response to the E2 epitope, we searched in particular for scaffolds of small size that would also accommodate antibody binding to the grafted epitope. We found that several structures corresponding to human α-defensins, which are antimicrobial peptides (approximately 30 amino acids in length) of the innate immune system, were optimal in this regard (Fig. 1B).

With a human α-defensin protein identified as a potential scaffold, we searched a set of all defensin structures for further candidate scaffolds in that family of proteins. This was due to experimentally observed self-association of the α-defensins (despite its monomeric bioassembly in the PDB), which are reported to form symmetric dimers via backbone-mediated interactions between β strands of the monomers (40); based on the location of the dimerization interface (41), HCV1 mAb binding would be blocked were the dimerization to take place in the context of the

grafted epitope. We identified another class of defensins, θ-defensins, that features a nearly identical β hairpin substructure as α-defensins, yet don't appear to stably self-associate (42). These were not part of the original search set as all available θ-defensin structures were determined by solution NMR rather than x-ray crystallography. As with α-defensins, they include three disulfide bonds, yet functional and structural characterization by NMR has shown that only one of the disulfide bonds is needed for structure and antimicrobial function (43). Based on the capability of these small (18 residue) cyclic peptides to form stable β hairpin structures nearly identical to the HCV1-bound epitope structure (Fig. 1C), with 0.9 Å average backbone RMSD among 20 NMR models, we generated two cyclic peptide designs (Fig. 1D) comprising minimal scaffolded structures of this epitope.

Design of a bivalent E2-based antigen. While a high resolution structure of the full E2 glycoprotein has yet to be experimentally described, two crystallographic structures of E2 core are available (7, 44); these correspond to engineered truncated variants of E2 from two genotypes. These structures have a shared globular fold, stabilized by numerous disulfide bonds, and epitope I, located near the N-terminus of E2, is fully or mostly absent from both structures. Analysis of these structures revealed a distinctive β hairpin at the same location on their surfaces, consisting of residues 625-644 (H77 isolate numbering); in one of the two E2 core structures, this site is directly engaged by an antibody (44). Given its high structural similarity to epitope I (0.8 Å backbone RMSD) as well as its surface accessibility, we engineered the E2 glycoprotein to display epitope I at this site, resulting in a bivalent E2-based scaffold with two copies of epitope I on its surface (Fig. 2). This was performed in the context of a truncated E2 construct, where we removed most of hypervariable region 1 (HVR1), given its immunogenicity and

capacity to mutate (45), as well as C-terminal residues that were disordered in the E2 core crystal structure. This protein, named Truncation 2 (T2), was tested alongside two control antigens, in addition to $E2_{661}$ (Fig. 2C): Truncation 1 (T1), corresponding to wild-type H77 E2 residues 409-645 (without the engineered epitope at aa 629-640), and Truncation 3 (T3) with the engineered epitope I at aa 629-640 and residues 409-423 removed.

Antibody binding of designed immunogens. Cyclic epitope I designs were synthesized and tested for binding to the HCV1 mAb using surface plasmon resonance (SPR; Fig. 3), to confirm epitope integrity in the context of the cyclization. Though antibody immobilization and peptide analyte was tested, this did not produce sufficient binding signals for analysis, therefore immobilized peptide and HCV1 mAb analyte were used for SPR assays. Both cyclic designs bound HCV1 with measurable affinities, comparable to the linear peptide (within experimental uncertainty), thus cyclization maintained the capability of these immunogens to engage HCV1.

To characterize the epitope presentation of the E2 constructs, $E2_{661}$ and E2 designs were engineered with a 6xHis fusion tag, expressed in HEK-293T cells and purified by nickel-affinity chromatography. All three truncated E2 designs were expressed at the expected size (Fig. 4). We tested antibody binding in ELISA using HCV1 as well as two other neutralizing antibodies, 95-2 and 96-2 (Fig. 5). Antibody 95-2 is related to HCV1 and binds epitope I (21), while 96-2 binds epitope II (aa 432-443) (25); as with HCV1, both were generated using immunization of $E2_{661}$ in mice engineered to express human antibodies (HuMAb, Medarex, Inc.). All antibodies were engaged by truncated E2 designs T1-T3, and though there was some (< 10-fold) variability in binding to HCV1, binding to 95-2 and 96-2 was more uniform. As no major loss of binding was

observed for any of the designed constructs, presentation of epitope I, as well as the epitope II site, was not disrupted in the context of these E2-based designs.

Structural characterization of cyclic C1 immunogen bound to HCV1. To confirm the structure of the designed C1 immunogen, we performed x-ray crystallography to determine its structure in complex with HCV1 (Fig. 6, Table 1). This structure was determined at 2.26 Å resolution, and deposited in the PDB under accession code 5KZP. A careful comparison of our HCV1-C1 complex structure with the structure of the HCV1 Fab bound to the linear E2 peptide (PDB code 4DGY (6)) reveals preserved binding mode and epitope conformation, as well as densities for the engineered disulfide bond and C-terminal lysine residue (K425) in the C1 peptide. As predicted, we observed no difference in the interface between HCV1 and C1 versus the interface between HCV1 and the linear peptide. We did observe a shift in the conformation of the HCV1 CDR H3 loop in the HCV1-C1 complex crystal structure (Fig. 6G, 6H), suggesting possible conformational dynamics of that loop; this may additionally be attributed to altered loop context in the crystallographic lattices of these two structures. After superposition of antibody variable (Fv) domains of these complexes, RMSDs between linear and C1 peptides confirm conservation of the epitope structure and binding orientation: 0.37-0.48 Å for epitope backbone atoms and 0.83-1.09 Å for all epitope atoms (ranges represent values from separate calculations using each of the four asymmetric units of the HCV1-C1 structure), with the larger values for the latter due primarily to Q412, N417, and N423 side chains which are exposed and not directly engaged by the antibody.

Serum antibody response elicited by designed antigens. To compare the antibody response elicited by engineered epitope I and E2-based antigens, we immunized mice with the two cyclic epitope I peptides and three truncated E2 antigens, alongside control antigens $E2_{661}$ and linear epitope I. Groups of CD1 mice (n=4) were immunized with 50 μg of the peptides or purified E2-based proteins, followed by four 10 μg boosts of over approximately six weeks. Soluble E2 ($E2_{661}$) was included as a positive control based on its previously described immunogenicity (21). Serum samples were collected one week after the fifth immunization, and sera from immunized mice were tested for epitope I-specific antibody response using ELISA (Fig. 7). Mice immunized with the cyclic antigens (C1, C2) showed strong ELISA reactivity against the epitope I peptide, whereas immunization of the linear peptides resulted in significantly lower serum response. The $E2_{661}$, T1 (truncated wild-type E2), and T2 (bivalent E2) antigens induced epitope-specific responses comparable to the cyclized peptides, with some variability among mice within each group. The T3 antigen, with the native epitope I site removed, induced the lowest epitope-specific responses among E2-based constructs, indicating that the transplanted epitope at aa 629-640 is lower in immunogenicity, or antibodies induced by that site don't cross react with the native epitope.

Viral neutralization. To determine if the immunized sera could neutralize virus *in vitro*, HCV pseudoparticle (HCVpp) neutralization assays were performed. Mouse sera were tested against HCVpp with H77 E1E2 sequences (Fig. 8, Table 2). Immunization with either cyclic peptide yielded measurable levels of neutralizing antibodies, with some variability within each group. However, no detectable neutralizing antibodies were generated in mice immunized with linear peptides, indicating that the engineered cyclic variants are superior immunogens. Mice

immunized with the E2-based antigens yielded higher neutralizing antibody responses than the peptide antigens, likely due to the presence of additional epitopes outside of epitope I capable of inducing neutralizing antibodies (46, 47), though as noted by others at least one such region, corresponding to epitope II which is targeted by the 96-2 mAb, is associated with viral escape (48). Among these antigens, $E2_{661}$ and T1 induced the highest levels of H77 neutralizing antibodies, with T2 and T3 constructs containing the transplanted epitope at aa 629-640 yielding lower neutralizing antibody responses.

To assess neutralization breadth, we tested serum neutralization using HCVpp derived from genotype 1b and 4a isolates (Table 2), which were used previously to characterize HCV1 mAb neutralization (21). For all constructs, neutralization activity against these was lower than for H77, suggesting limited neutralization breadth overall. The T1 design maintained the neutralization of the genotype 1b HCVpp with respect to $E2_{661}$, with possible modest improvement. For the designed cyclic constructs, neutralization breadth was limited, suggesting that despite robust epitope I-specific responses, limited sequence variability within the epitope (I414V for the 1b isolate, T416S for the 4a isolate (21)), or other variations in viral sequence or fitness reduced the neutralization capacity of immunized sera against these isolates.

DISCUSSION

The area of structure-based HCV vaccine design has seen limited success recently reported by others. One study described structure-based design of scaffolded antigens for HCV to display an E1 epitope as well as E2 epitope I (49). Though the latter constructs were tested for binding to the HCV1 antibody, no in vivo results were reported. The designs resulting from the meta-server

355 methodology described in that study were larger and distinct from the cyclic designs we
356 produced and tested in vivo. More recently, a study was reported featuring a cyclic epitope I
357 construct with a different mode of disulfide cyclization than C1 or C2, including epitope residues
358 412-422 rather than 412-423 (C1) or 409-425 (C2), and no glycan at N417 (50). After murine
359 immunization with this antigen, several elicited mAbs were tested for epitope binding and
360 neutralization, but no measurable neutralization was observed. By employing two distinct design
361 approaches, scaffolding of the epitope to present the stabilized epitope structure to the immune
362 system (C1, C2), and antigen redesign (T1, T2, T3), we were able to provide an unprecedented
363 comparison of these widely different design strategies in vivo for their potential to elicit epitope-
364 specific and neutralizing antibodies to HCV, along with structural characterization of a designed
365 immunogen.
366
367 Although the bivalent E2 construct we produced (T2) yielded lower neutralizing antibody
368 responses than the monovalent control (T1) based on H77 ID50 values (Table 1), further
369 exploration of this approach may be warranted. One advantage of this bivalent antigen not
370 considered in the design strategy was the disruption via mutation of an E2 epitope associated
371 with non-neutralizing antibodies that includes residue Y632 (28). Furthermore, the absence of
372 HVR1 in T2 and other truncated constructs is an advantage over $E2_{661}$, as that region is
373 associated with high sequence variability and escape from neutralizing antibodies (45). However,
374 its reduced capacity to induce neutralizing antibodies, and no apparent improvement in levels of
375 epitope I-specific antibodies, suggests that the T2 antigen requires further design to improve
376 presentation of the transplanted epitope, and possibly its stability. One option in this regard
377 would be design to optimize the E2 core-epitope interface at aa 629-640, which was not

performed originally in order to preserve the full epitope sequence. Such designs could include removal of the glycan at epitope position N417 via mutation of N417 or S419, in conjunction with other substitutions of non-HCV1 contact residues proximal to E2 core to improve packing and shape complementarity. Intriguingly, others have recently noted that for another truncated variant of E2 (with HVRs 1-3 removed), high molecular weight forms of the protein improve neutralizing antibody responses, thus providing an additional route to increase neutralization potency and breadth of these E2-based designs (51). While we did observe epitope I-specific and neutralizing antibodies elicited by our truncated designs, epitope II and other sites on E2 may indeed be targeted by the neutralizing response; the extent of epitope I-specific neutralizing antibodies can possibly be probed in future work through additional assays such as inhibition of HCVpp neutralization using epitope I peptide.

The cyclic antigens we generated highlight the potential of minimal stabilized antigens to induce neutralizing epitope-specific antibodies that improve over immunization with the linear peptide. The improvement in immunogenicity does not seem to be due to improved HCV1 binding affinity, as based on our assays there was no significant change, though other binding assays such as isothermal titration calorimetry may help to confirm this. As at least one extended epitope I structure is associated with an antibody with relatively weak neutralization (12), and cyclization would avoid or disfavor such a conformation, it is possible that constraining the epitope conformation could affect the quality of antibody response. However, given the improvement in epitope-specific antibody titers from cyclic designs, other factors, such as improved serum stability and half-life of the cyclic designs, may be responsible. Though the levels of neutralizing antibodies induced by the cyclic epitopes were relatively low, compared

401 with $E2_{661}$ immunized sera, and exhibited limited neutralization breadth, a number of options are
402 available to improve neutralizing antibody response, including display of the cyclic immunogens
403 on virus-like particles or nanoparticles (52). Heterologous prime-boost vaccination, with E2 or
404 E1E2 protein as prime, followed by boost with cyclic epitope I to focus the response to that
405 portion of E2, as utilized by others for HIV vaccination (53), may also improve levels of epitope
406 I-specific neutralizing antibodies.
407
408 The limited neutralization breadth elicited by the cyclic constructs is possibly related to recent
409 observations of HCV neutralization where certain isolates exhibit broad nAb resistance, which
410 was correlated with overall viral infectivity for a large panel of HCVpp (54). In another study,
411 non-epitope E2 residues affecting co-receptor binding appeared to be responsible for resistance
412 (55), while others have noted variability in neutralization with mAbs targeting epitope I, despite
413 conserved epitope sequence (22). A deep sequencing analysis of patients undergoing HCV1
414 mAb immunotherapy revealed E1 and E2 positions outside of epitope I with relatively high
415 mutation rates, suggesting a possible direct or indirect role in evading antibody targeting of that
416 epitope (56). In light of the relatively low but detectable levels of H77 neutralization, it is
417 possible that even modest (2-4 fold) increase in resistance in the 1b and 4a HCVpp tested led to
418 lack of measurable neutralization in the case of the cyclic peptide-immunized sera, and
419 modifications in immunogen display as noted above would lead to more detectable and robust
420 neutralization breadth. HCVpp representing a larger set of isolates can be included in follow-up
421 studies of these designs to provide more support of neutralization breadth or lack thereof.
422

Further design of the cyclic constructs may also yield improved responses. Characterization of mAbs induced by C1 or C2 vaccination, via alanine scanning mutagenesis, affinity measurements, or crystallography, may yield information regarding the induced repertoire and possible molecular details underlying the observed difference between epitope I-specific binding and neutralization, for instance mAb binding to portions of the epitope that are inaccessible in the context of E2 or the virion. Such characterization of C1 and C2-elicited mAbs, which was utilized recently for another cyclic epitope I design as noted above (50), could indicate the basis of neutralization in immunized sera from our constructs and inform second-generation designs of one or both of those antigens. Additionally, as glycosylation or mutation at position N415 is associated with escape from HCV1 (25, 56) and other mAbs (9), addition of a glycan at position N415, in addition to N417, may induce antibodies capable of targeting this epitope with a binding footprint that does not include N415, while maintaining binding to the conserved residues L413 and W420. Given the glycan sequons of NxT and NxS, simultaneous glycosylation at N415 and N417 is only possible in a synthetic peptide (such as the ones described here) rather than an expressed protein antigen. Recently described structural characterization of an epitope I-targeting mAb, HC33.1, that can neutralize the glycan-shifted N417S variant and engages the epitope in a unique extended conformation, may lead to additional scaffolded or stabilized designed antigens (30). We have shown here, using the HCV1-bound epitope I conformation, that such an approach is possible and merits further investigation.

ACKNOWLEDGEMENTS

We would like to thank Mark S. Klempner (MassBiologics) for useful suggestions on study design, as well as Steven K. H. Foung and Zhenyong Keck (Stanford University School of Medicine) for their comments. We would additionally like to thank Bob Beadenkopf for outstanding technical assistance and the beamline support staff at Stanford Synchrotron Radiation Lightsource and Advanced Photon Source.

Research reported in this publication was supported by the National Center for Advancing Translational Sciences of the NIH under award number UL1-TR001453. B.G.P. was additionally supported through startup funding from the University of Maryland and NIH grant R21-AI126582. The content is solely the responsibility of the authors and does not necessarily represent the official views of the NIH.

459 **REFERENCES**

460 1. **Cox AL.** 2015. MEDICINE. Global control of hepatitis C virus. Science **349:**790-791.

461 2. **Lauer GM, Walker BD.** 2001. Hepatitis C virus infection. The New England journal of
462 medicine **345:**41-52.

463 3. **Dunlop J, Owsianka A, Cowton V, Patel A.** 2015. Current and future prophylactic
464 vaccines for hepatitis C virus. Vaccine: Development and Therapy **2015:**31-44.

465 4. **Halliday J, Klenerman P, Barnes E.** 2011. Vaccination for hepatitis C virus: closing in
466 on an evasive target. Expert Rev Vaccines **10:**659-672.

467 5. **Cashman SB, Marsden BD, Dustin LB.** 2014. The Humoral Immune Response to
468 HCV: Understanding is Key to Vaccine Development. Front Immunol **5:**550.

469 6. **Kong L, Giang E, Robbins JB, Stanfield RL, Burton DR, Wilson IA, Law M.** 2012.
470 Structural basis of hepatitis C virus neutralization by broadly neutralizing antibody
471 HCV1. Proceedings of the National Academy of Sciences of the United States of
472 America **109:**9499-9504.

473 7. **Kong L, Giang E, Nieusma T, Kadam RU, Cogburn KE, Hua Y, Dai X, Stanfield**
474 **RL, Burton DR, Ward AB, Wilson IA, Law M.** 2013. Hepatitis C virus E2 envelope
475 glycoprotein core structure. Science **342:**1090-1094.

476 8. **Kong L, Giang E, Nieusma T, Robbins JB, Deller MC, Stanfield RL, Wilson IA,**
477 **Law M.** 2012. Structure of Hepatitis C Virus Envelope Glycoprotein E2 Antigenic Site
478 412 to 423 in Complex with Antibody AP33. J Virol **86:**13085-13088.

479 9. **Pantua H, Diao J, Ultsch M, Hazen M, Mathieu M, McCutcheon K, Takeda K, Date**
480 **S, Cheung TK, Phung Q, Hass P, Arnott D, Hongo JA, Matthews DJ, Brown A,**
481 **Patel AH, Kelley RF, Eigenbrot C, Kapadia SB.** 2013. Glycan shifting on hepatitis C

virus (HCV) E2 glycoprotein is a mechanism for escape from broadly neutralizing antibodies. J Mol Biol **425:**1899-1914.

10. **Deng L, Zhong L, Struble E, Duan H, Ma L, Harman C, Yan H, Virata-Theimer ML, Zhao Z, Feinstone S, Alter H, Zhang P.** 2013. Structural evidence for a bifurcated mode of action in the antibody-mediated neutralization of hepatitis C virus. Proc Natl Acad Sci U S A **110:**7418-7422.

11. **Krey T, Meola A, Keck ZY, Damier-Piolle L, Foung SK, Rey FA.** 2013. Structural basis of HCV neutralization by human monoclonal antibodies resistant to viral neutralization escape. PLoS Pathog **9:**e1003364.

12. **Meola A, Tarr AW, England P, Meredith LW, McClure CP, Foung SK, McKeating JA, Ball JK, Rey FA, Krey T.** 2015. Structural flexibility of a conserved antigenic region in hepatitis C virus glycoprotein E2 recognized by broadly neutralizing antibodies. J Virol **89:**2170-2181.

13. **Kong L, Kadam RU, Giang E, Ruwona TB, Nieusma T, Culhane JC, Stanfield RL, Dawson PE, Wilson IA, Law M.** 2015. Structure of Hepatitis C Virus Envelope Glycoprotein E1 Antigenic Site 314-324 in Complex with Antibody IGH526. J Mol Biol **427:**2617-2628.

14. **Kong L, Jackson KN, Wilson IA, Law M.** 2015. Capitalizing on knowledge of hepatitis C virus neutralizing epitopes for rational vaccine design. Curr Opin Virol **11:**148-157.

15. **Ofek G, Guenaga FJ, Schief WR, Skinner J, Baker D, Wyatt R, Kwong PD.** 2010. Elicitation of structure-specific antibodies by epitope scaffolds. Proceedings of the National Academy of Sciences of the United States of America **107:**17880-17887.

16. **Jardine J, Julien JP, Menis S, Ota T, Kalyuzhniy O, McGuire A, Sok D, Huang PS, MacPherson S, Jones M, Nieusma T, Mathison J, Baker D, Ward AB, Burton DR, Stamatatos L, Nemazee D, Wilson IA, Schief WR.** 2013. Rational HIV immunogen design to target specific germline B cell receptors. Science **340:**711-716.

17. **Yassine HM, Boyington JC, McTamney PM, Wei CJ, Kanekiyo M, Kong WP, Gallagher JR, Wang L, Zhang Y, Joyce MG, Lingwood D, Moin SM, Andersen H, Okuno Y, Rao SS, Harris AK, Kwong PD, Mascola JR, Nabel GJ, Graham BS.** 2015. Hemagglutinin-stem nanoparticles generate heterosubtypic influenza protection. Nat Med **21:**1065-1070.

18. **Impagliazzo A, Milder F, Kuipers H, Wagner MV, Zhu X, Hoffman RM, van Meersbergen R, Huizingh J, Wanningen P, Verspuij J, de Man M, Ding Z, Apetri A, Kukrer B, Sneekes-Vriese E, Tomkiewicz D, Laursen NS, Lee PS, Zakrzewska A, Dekking L, Tolboom J, Tettero L, van Meerten S, Yu W, Koudstaal W, Goudsmit J, Ward AB, Meijberg W, Wilson IA, Radosevic K.** 2015. A stable trimeric influenza hemagglutinin stem as a broadly protective immunogen. Science **349:**1301-1306.

19. **McLellan JS, Chen M, Joyce MG, Sastry M, Stewart-Jones GB, Yang Y, Zhang B, Chen L, Srivatsan S, Zheng A, Zhou T, Graepel KW, Kumar A, Moin S, Boyington JC, Chuang GY, Soto C, Baxa U, Bakker AQ, Spits H, Beaumont T, Zheng Z, Xia N, Ko SY, Todd JP, Rao S, Graham BS, Kwong PD.** 2013. Structure-based design of a fusion glycoprotein vaccine for respiratory syncytial virus. Science **342:**592-598.

20. **Correia BE, Bates JT, Loomis RJ, Baneyx G, Carrico C, Jardine JG, Rupert P, Correnti C, Kalyuzhniy O, Vittal V, Connell MJ, Stevens E, Schroeter A, Chen M, Macpherson S, Serra AM, Adachi Y, Holmes MA, Li Y, Klevit RE, Graham BS,**

527 **Wyatt RT, Baker D, Strong RK, Crowe JE, Jr., Johnson PR, Schief WR.** 2014. Proof
528 of principle for epitope-focused vaccine design. Nature **507:**201-206.
529 21. **Broering TJ, Garrity KA, Boatright NK, Sloan SE, Sandor F, Thomas WD, Jr.,**
530 **Szabo G, Finberg RW, Ambrosino DM, Babcock GJ.** 2009. Identification and
531 characterization of broadly neutralizing human monoclonal antibodies directed against
532 the E2 envelope glycoprotein of hepatitis C virus. J Virol **83:**12473-12482.
533 22. **Keck Z, Wang W, Wang Y, Lau P, Carlsen TH, Prentoe J, Xia J, Patel AH, Bukh J,**
534 **Foung SK.** 2013. Cooperativity in virus neutralization by human monoclonal antibodies
535 to two adjacent regions located at the amino terminus of hepatitis C virus E2
536 glycoprotein. J Virol **87:**37-51.
537 23. **Tarr AW, Owsianka AM, Timms JM, McClure CP, Brown RJ, Hickling TP,**
538 **Pietschmann T, Bartenschlager R, Patel AH, Ball JK.** 2006. Characterization of the
539 hepatitis C virus E2 epitope defined by the broadly neutralizing monoclonal antibody
540 AP33. Hepatology **43:**592-601.
541 24. **Sabo MC, Luca VC, Prentoe J, Hopcraft SE, Blight KJ, Yi M, Lemon SM, Ball JK,**
542 **Bukh J, Evans MJ, Fremont DH, Diamond MS.** 2011. Neutralizing monoclonal
543 antibodies against hepatitis C virus E2 protein bind discontinuous epitopes and inhibit
544 infection at a postattachment step. J Virol **85:**7005-7019.
545 25. **Morin TJ, Broering TJ, Leav BA, Blair BM, Rowley KJ, Boucher EN, Wang Y,**
546 **Cheslock PS, Knauber M, Olsen DB, Ludmerer SW, Szabo G, Finberg RW, Purcell**
547 **RH, Lanford RE, Ambrosino DM, Molrine DC, Babcock GJ.** 2012. Human
548 Monoclonal Antibody HCV1 Effectively Prevents and Treats HCV Infection in
549 Chimpanzees. PLoS pathogens **8:**e1002895.

26. **Chung RT, Gordon FD, Curry MP, Schiano TD, Emre S, Corey K, Markmann JF, Hertl M, Pomposelli JJ, Pomfret EA, Florman S, Schilsky M, Broering TJ, Finberg RW, Szabo G, Zamore PD, Khettry U, Babcock GJ, Ambrosino DM, Leav B, Leney M, Smith HL, Molrine DC.** 2013. Human monoclonal antibody MBL-HCV1 delays HCV viral rebound following liver transplantation: a randomized controlled study. Am J Transplant **13:**1047-1054.

27. **Ball JK, Tarr AW, McKeating JA.** 2014. The past, present and future of neutralizing antibodies for hepatitis C virus. Antiviral Res **105:**100-111.

28. **Pierce BG, Keck ZY, Lau P, Fauvelle C, Gowthaman R, Baumert TF, Fuerst TR, Mariuzza RA, Foung SK.** 2016. Global mapping of antibody recognition of the hepatitis C virus E2 glycoprotein: Implications for vaccine design. Proc Natl Acad Sci U S A doi:10.1073/pnas.1614942113.

29. **Tarr AW, Owsianka AM, Jayaraj D, Brown RJ, Hickling TP, Irving WL, Patel AH, Ball JK.** 2007. Determination of the human antibody response to the epitope defined by the hepatitis C virus-neutralizing monoclonal antibody AP33. J Gen Virol **88:**2991-3001.

30. **Li Y, Pierce BG, Wang Q, Keck ZY, Fuerst TR, Foung SK, Mariuzza RA.** 2015. Structural basis for penetration of the glycan shield of hepatitis C virus E2 glycoprotein by a broadly neutralizing human antibody. J Biol Chem **290:**10117-10125.

31. **Berman HM, Westbrook J, Feng Z, Gilliland G, Bhat TN, Weissig H, Shindyalov IN, Bourne PE.** 2000. The Protein Data Bank. Nucleic Acids Res **28:**235-242.

32. **Zhu J, Weng Z.** 2005. FAST: a novel protein structure alignment algorithm. Proteins **58:**618-627.

33. **Collaborative Computational Project N.** 1994. The CCP4 suite: programs for protein crystallography. Acta Crystallogr D Biol Crystallogr **50:**760-763.

34. **Adams PD, Afonine PV, Bunkoczi G, Chen VB, Echols N, Headd JJ, Hung LW, Jain S, Kapral GJ, Grosse Kunstleve RW, McCoy AJ, Moriarty NW, Oeffner RD, Read RJ, Richardson DC, Richardson JS, Terwilliger TC, Zwart PH.** 2011. The Phenix software for automated determination of macromolecular structures. Methods **55:**94-106.

35. **McCoy AJ, Grosse-Kunstleve RW, Adams PD, Winn MD, Storoni LC, Read RJ.** 2007. Phaser crystallographic software. J Appl Crystallogr **40:**658-674.

36. **Emsley P, Cowtan K.** 2004. Coot: model-building tools for molecular graphics. Acta crystallographica Section D, Biological crystallography **60:**2126-2132.

37. **Kleiger G, Saha A, Lewis S, Kuhlman B, Deshaies RJ.** 2009. Rapid E2-E3 assembly and disassembly enable processive ubiquitylation of cullin-RING ubiquitin ligase substrates. Cell **139:**957-968.

38. **Owsianka A, Tarr AW, Juttla VS, Lavillette D, Bartosch B, Cosset FL, Ball JK, Patel AH.** 2005. Monoclonal antibody AP33 defines a broadly neutralizing epitope on the hepatitis C virus E2 envelope glycoprotein. J Virol **79:**11095-11104.

39. **Kuiken C, Yusim K, Boykin L, Richardson R.** 2005. The Los Alamos hepatitis C sequence database. Bioinformatics **21:**379-384.

40. **Pazgier M, Wei G, Ericksen B, Jung G, Wu Z, de Leeuw E, Yuan W, Szmacinski H, Lu WY, Lubkowski J, Lehrer RI, Lu W.** 2012. Sometimes it takes two to tango: contributions of dimerization to functions of human alpha-defensin HNP1 peptide. J Biol Chem **287:**8944-8953.

41. **Wei G, de Leeuw E, Pazgier M, Yuan W, Zou G, Wang J, Ericksen B, Lu WY, Lehrer RI, Lu W.** 2009. Through the looking glass, mechanistic insights from enantiomeric human defensins. J Biol Chem **284:**29180-29192.

42. **Conibear AC, Rosengren KJ, Harvey PJ, Craik DJ.** 2012. Structural characterization of the cyclic cystine ladder motif of theta-defensins. Biochemistry **51:**9718-9726.

43. **Conibear AC, Rosengren KJ, Daly NL, Henriques ST, Craik DJ.** 2013. The cyclic cystine ladder in theta-defensins is important for structure and stability, but not antibacterial activity. J Biol Chem **288:**10830-10840.

44. **Khan AG, Whidby J, Miller MT, Scarborough H, Zatorski AV, Cygan A, Price AA, Yost SA, Bohannon CD, Jacob J, Grakoui A, Marcotrigiano J.** 2014. Structure of the core ectodomain of the hepatitis C virus envelope glycoprotein 2. Nature **509:**381-384.

45. **Pierce BG, Keck ZY, Foung SK.** 2016. Viral evasion and challenges of hepatitis C virus vaccine development. Curr Opin Virol **20:**55-63.

46. **Keck ZY, Li TK, Xia J, Gal-Tanamy M, Olson O, Li SH, Patel AH, Ball JK, Lemon SM, Foung SK.** 2008. Definition of a conserved immunodominant domain on hepatitis C virus E2 glycoprotein by neutralizing human monoclonal antibodies. J Virol **82:**6061-6066.

47. **Keck ZY, Xia J, Wang Y, Wang W, Krey T, Prentoe J, Carlsen T, Li AY, Patel AH, Lemon SM, Bukh J, Rey FA, Foung SK.** 2012. Human monoclonal antibodies to a novel cluster of conformational epitopes on HCV E2 with resistance to neutralization escape in a genotype 2a isolate. PLoS Pathog **8:**e1002653.

48. **Keck ZY, Saha A, Xia J, Wang Y, Lau P, Krey T, Rey FA, Foung SK.** 2011. Mapping a region of hepatitis C virus E2 that is responsible for escape from neutralizing

antibodies and a core CD81-binding region that does not tolerate neutralization escape mutations. J Virol **85:**10451-10463.

49. **He L, Cheng Y, Kong L, Azadnia P, Giang E, Kim J, Wood MR, Wilson IA, Law M, Zhu J.** 2015. Approaching rational epitope vaccine design for hepatitis C virus with meta-server and multivalent scaffolding. Sci Rep **5:**12501.

50. **Sandomenico A, Leonardi A, Berisio R, Sanguigno L, Foca G, Foca A, Ruggiero A, Doti N, Muscariello L, Barone D, Farina C, Owsianka A, Vitagliano L, Patel AH, Ruvo M.** 2016. Generation and Characterization of Monoclonal Antibodies against a Cyclic Variant of Hepatitis C Virus E2 Epitope 412-422. J Virol **90:**3745-3759.

51. **Vietheer PT, Boo I, Gu J, McCaffrey K, Edwards S, Owczarek C, Hardy MP, Fabri L, Center RJ, Poumbourios P, Drummer HE.** 2017. The core domain of hepatitis C virus glycoprotein E2 generates potent cross-neutralizing antibodies in guinea pigs. Hepatology **65:**1117-1131.

52. **Zhao L, Seth A, Wibowo N, Zhao CX, Mitter N, Yu C, Middelberg AP.** 2014. Nanoparticle vaccines. Vaccine **32:**327-337.

53. **Walker LM, Burton DR.** 2010. Rational antibody-based HIV-1 vaccine design: current approaches and future directions. Curr Opin Immunol **22:**358-366.

54. **Urbanowicz RA, McClure CP, Brown RJ, Tsoleridis T, Persson MA, Krey T, Irving WL, Ball JK, Tarr AW.** 2015. A Diverse Panel of Hepatitis C Virus Glycoproteins for Use in Vaccine Research Reveals Extremes of Monoclonal Antibody Neutralization Resistance. J Virol **90:**3288-3301.

55. **El-Diwany R, Cohen VJ, Mankowski MC, Wasilewski LN, Brady JK, Snider AE, Osburn WO, Murrell B, Ray SC, Bailey JR.** 2017. Extra-epitopic hepatitis C virus

polymorphisms confer resistance to broadly neutralizing antibodies by modulating binding to scavenger receptor B1. PLoS Pathog **13:**e1006235.

56. **Babcock GJ, Iyer S, Smith HL, Wang Y, Rowley K, Ambrosino DM, Zamore PD, Pierce BG, Molrine DC, Weng Z.** 2014. High-throughput sequencing analysis of post-liver transplantation HCV E2 glycoprotein evolution in the presence and absence of neutralizing monoclonal antibody. PLoS One **9:**e100325.

FIGURE LEGENDS

Figure 1. Scaffold search and design of epitope I protein antigens. (A) Search of protein crystal structures for epitope I scaffolds. Antibody accessibility (clash of superposed epitope-bound HCV1 antibody structure with scaffold) versus protein size is shown for each candidate scaffold (scaffolds with higher antibody clash not shown in figure), with three α-defensin structures (PDB codes 1ZMM, 1ZMP, 1ZMQ) shown as red triangles. (B) Alignment of HCV1 bound E2 epitope I (PDB code 4DGY; green) to an NMR conformer of cyclic θ-defensin (PDB code 2M2S; cyan), which was engineered to remove two out of three internal disulfide bonds; HCV1 mAb (tan and light blue surface for heavy and light chains, respectively) is shown for reference. Backbone root-mean-square distance (RMSD) between epitope I and matching BTD-2 residues is 0.9 Å. Cyclic residues and those corresponding to key epitope positions L413, G418, and W420 are shown as sticks, with the epitope positions labeled. BTD-2 backbone cyclization is colored red, and disulfide bond is colored yellow. (B) Sequence of BTD-2, and tested linear and cyclic peptides, with cyclized residues colored as in (A), BTD-2 cysteines that were mutated in the NMR structure to remove disulfide bonds colored gray, and positions L413, G418 and W420

colored green. Linear and C2 constructs contain E2 residues 409-425, while C1 contains E2 residues 412-423; all tested peptides include a C-terminal lysine for carrier protein conjugation.

Figure 2. Design of an E2-based epitope I bivalent immunogen. (A) Structure of E2 core (PDB code 4MWF; magenta), aligned to HCV1-bound epitope I (PDB code 4DGY; green) using residues 629-640. HCV1 mAb (tan and light blue surface for heavy and light chains, respectively) is shown for reference. Epitope residues L413, G418 and W420, as well as corresponding E2 core residues R630, G635, and E637, are shown as sticks, and epitope positions are labeled. Backbone root-mean-square distance between epitope I and matching E2 core residues (aa 629-640) is 0.8 Å. (B) Model of HCV1 mAb bound to the native epitope I site on E2 (aa 412-423) as well as engineered epitope I site at aa 629-640, with both sites colored green, and E2 core and mAb colored as in (A). (C) Tested E2 constructs $E2_{661}$, T1 (truncated native), T2 (truncated bivalent), and T3 (truncated engineered site only), with E2 epitope I sequence locations represented as green boxes.

Figure 3. Binding of linear and cyclic peptides to the HCV1 mAb, measured by surface plasmon resonance. Peptides were coupled to bovine serum albumin and immobilized on the chip surface, and binding was measured using a two-fold dilution series of HCV1 mAb from 125-1.9 nM. Fitting of kinetic binding data (black lines) was performed using a bivalent analyte model, and calculated K_{D1} values, representing the initial 2:1 interaction affinities, are shown. Standard deviations were calculated from four independent experiments.

Figure 4. SDS-PAGE gel of purified T1, T2, T3, and $E2_{661}$ proteins. All proteins were treated with PNGase to remove glycans, which is the upper band (~36 kDa) in each lane (right-most

lane contains PNGase only). Reference sizes are shown on the left. Measured $E2_{661}$ and truncated E2 sizes range from 26-31 kDa, corresponding to expected protein sizes.

Figure 5. Binding of $E2_{661}$ and designed E2 proteins to neutralizing mAbs HCV1, 95-2, and 96-2 measured by ELISA. Error bars denote standard deviation from two independent experiments (performed for $E2_{661}$ only), and half-maximal binding titer (EC_{50}) was calculated for each interaction by curve fitting in GraphPad Prism software.

Figure 6. Structure of designed C1 immunogen bound to the HCV1 antibody. (A) The crystallographic structure of full HCV1-C1 complex (A), as well as details of the bound C1 peptide in side view (C), top view (E), and the HCV1 CDR loops (G), are shown in comparison with the structure of the native linear epitope bound to HCV1 (B, D, F, H) which was previously described (6) (PDB code 4DGY). Peptides are shown as green sticks (with oxygen atoms in red, nitrogen atoms in blue, and sulfur atoms in yellow) and HCV1 antibody is shown as cartoon with light chain colored light blue and heavy chain colored tan. Key epitope residues for HCV1 binding and β turn structure (L413, G418, W420), as well as terminal and cyclization residues, are labeled in (C) and (D), and selected HCV1 CDR loops are labeled in (G) and (H). In top view of epitope (E, F), side chains are omitted and intra-peptide hydrogen bonds are shown as black dashed lines.

Figure 7. Binding of immunized mouse sera to epitope I. Four mice per group were immunized with E2-based or peptide construct, and sera were tested using ELISA for binding to a linear epitope I peptide (aa 409-425, H77 sequence) conjugated to BSA, using a coating concentration of 2 μg/ml. P-values were calculated using a two-tailed t-test (***, $p \leq 0.001$; ns, not significant, $p > 0.05$).

Figure 8. HCV neutralization of immunized mouse sera. Four mice per group were immunized with E2-based or peptide construct, and sera were tested using the HCVpp assay for genotype 1a neutralization. The neutralization activity at 1:64 serum dilution was normalized with the activity of pre-immune serum and expressed as percentage of neutralization for each animal. Lines denote mean values for each group. P-values were calculated using a two-tailed t-test (*, $p \leq 0.05$; **, $p \leq 0.01$; ns, not significant, $p > 0.05$).

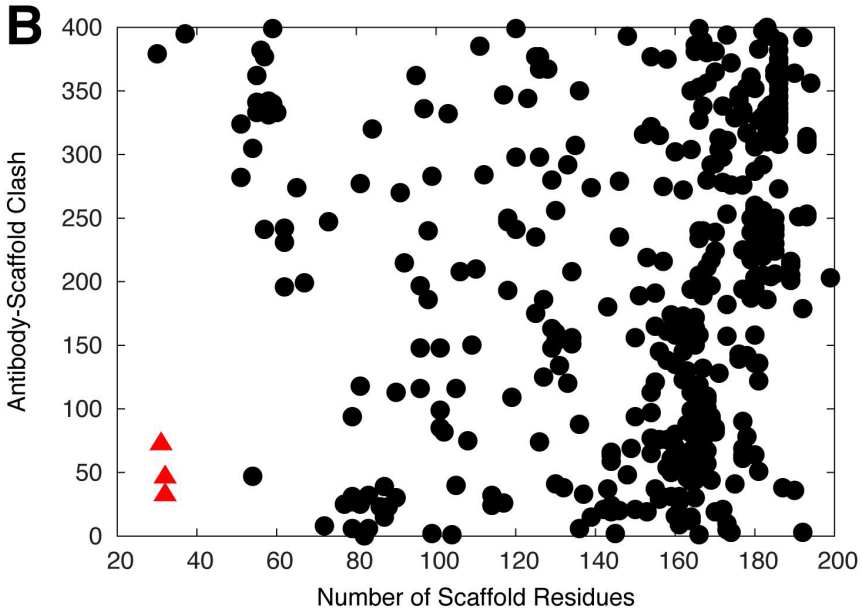

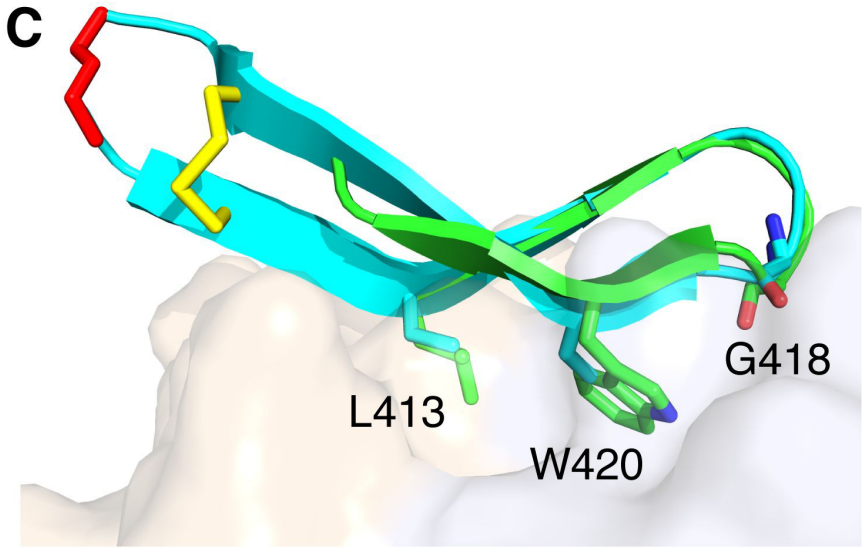

D

```
BTD-2   GVCRCVCRRGVCRCVCRR
linear  QNIQLINTNGSWHINSTK
C1        CQLINTNGSWHINCK
C2      QNIQLINTNGSWHINSTK
```

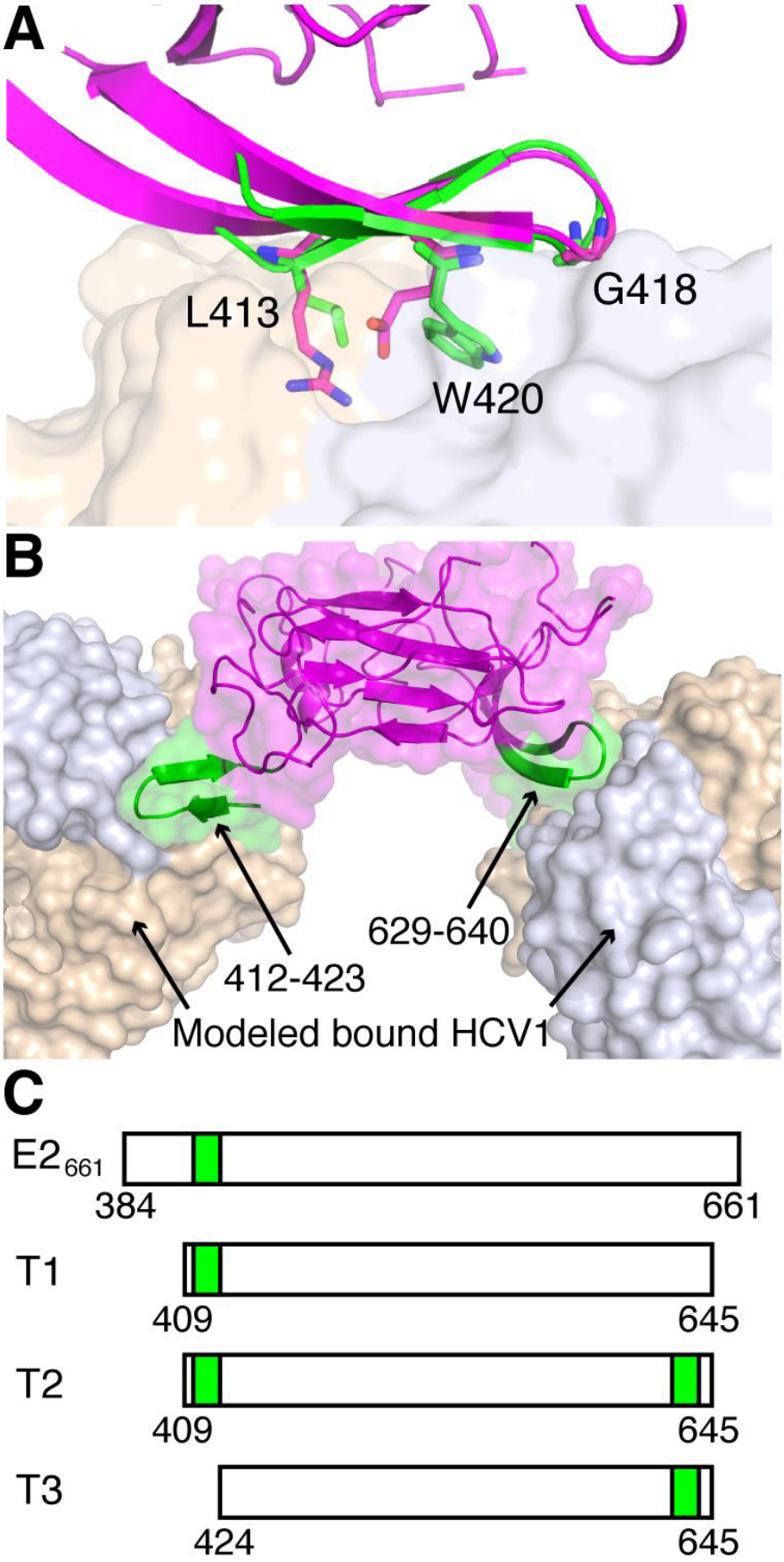

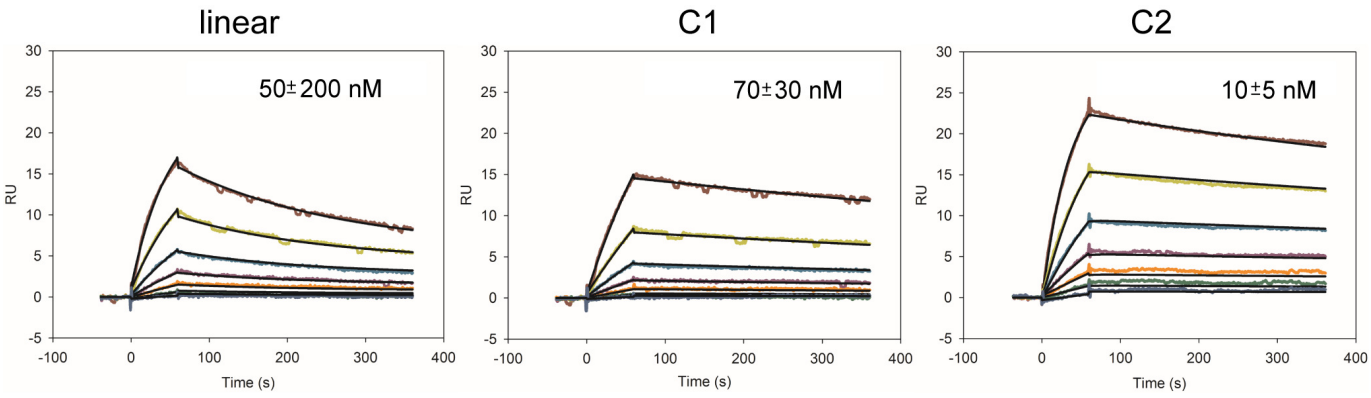

Journal of Virology

JVI

Journal of Virology

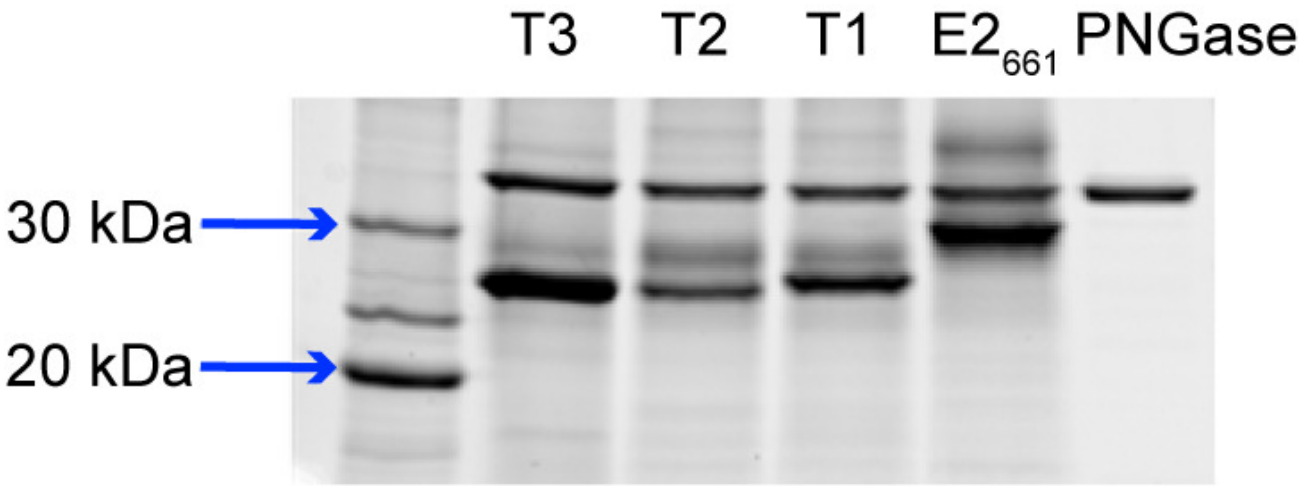

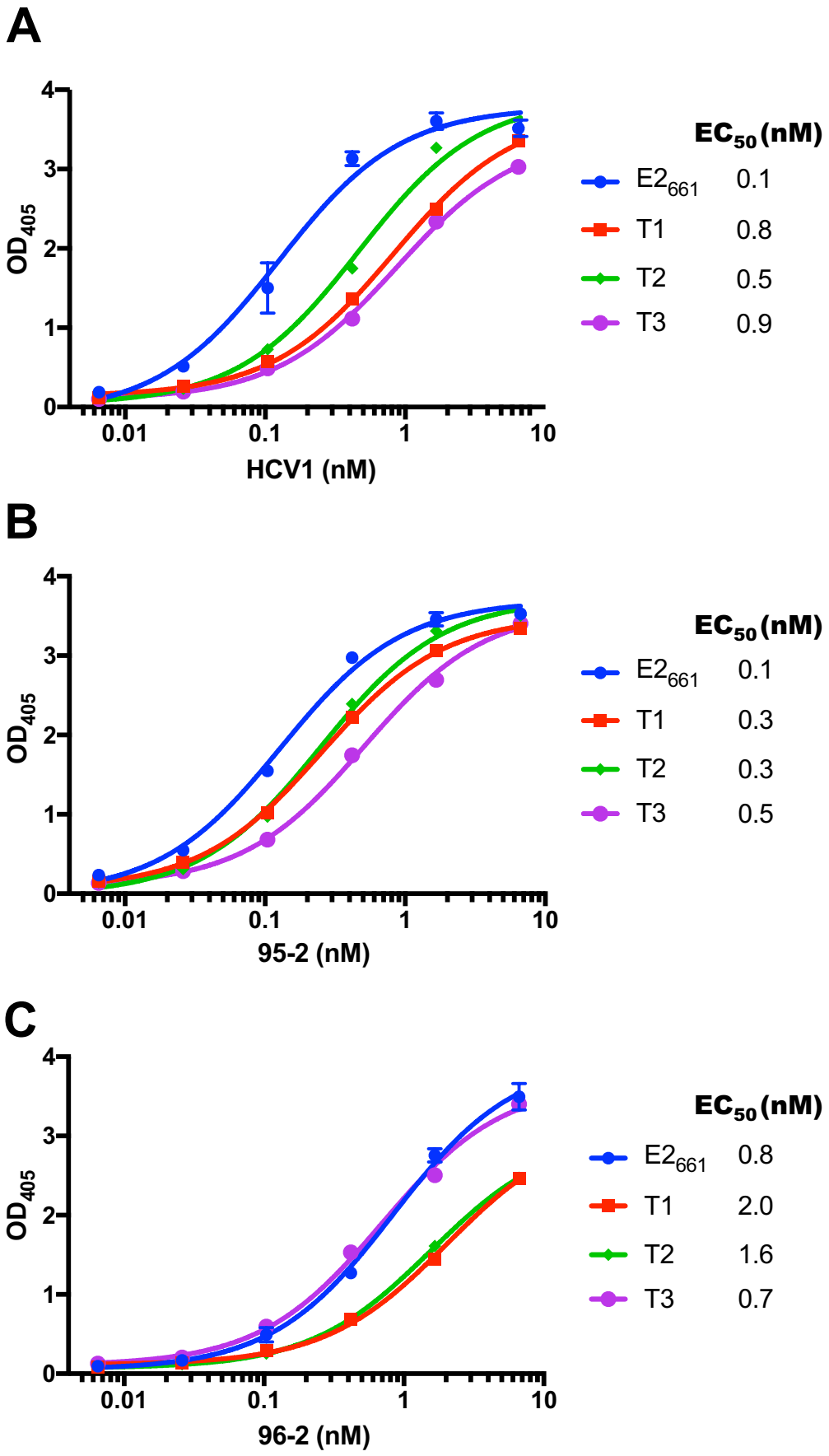

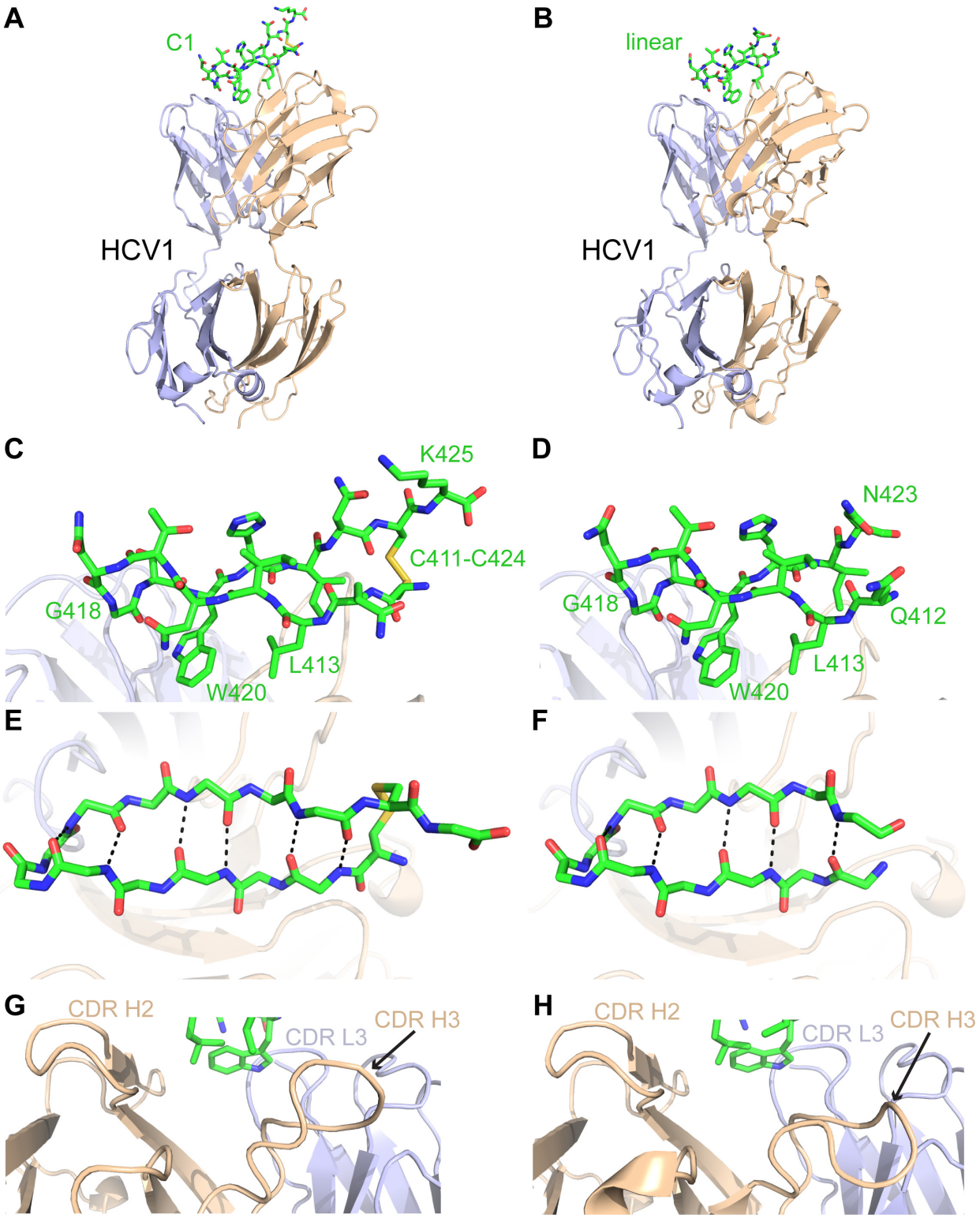

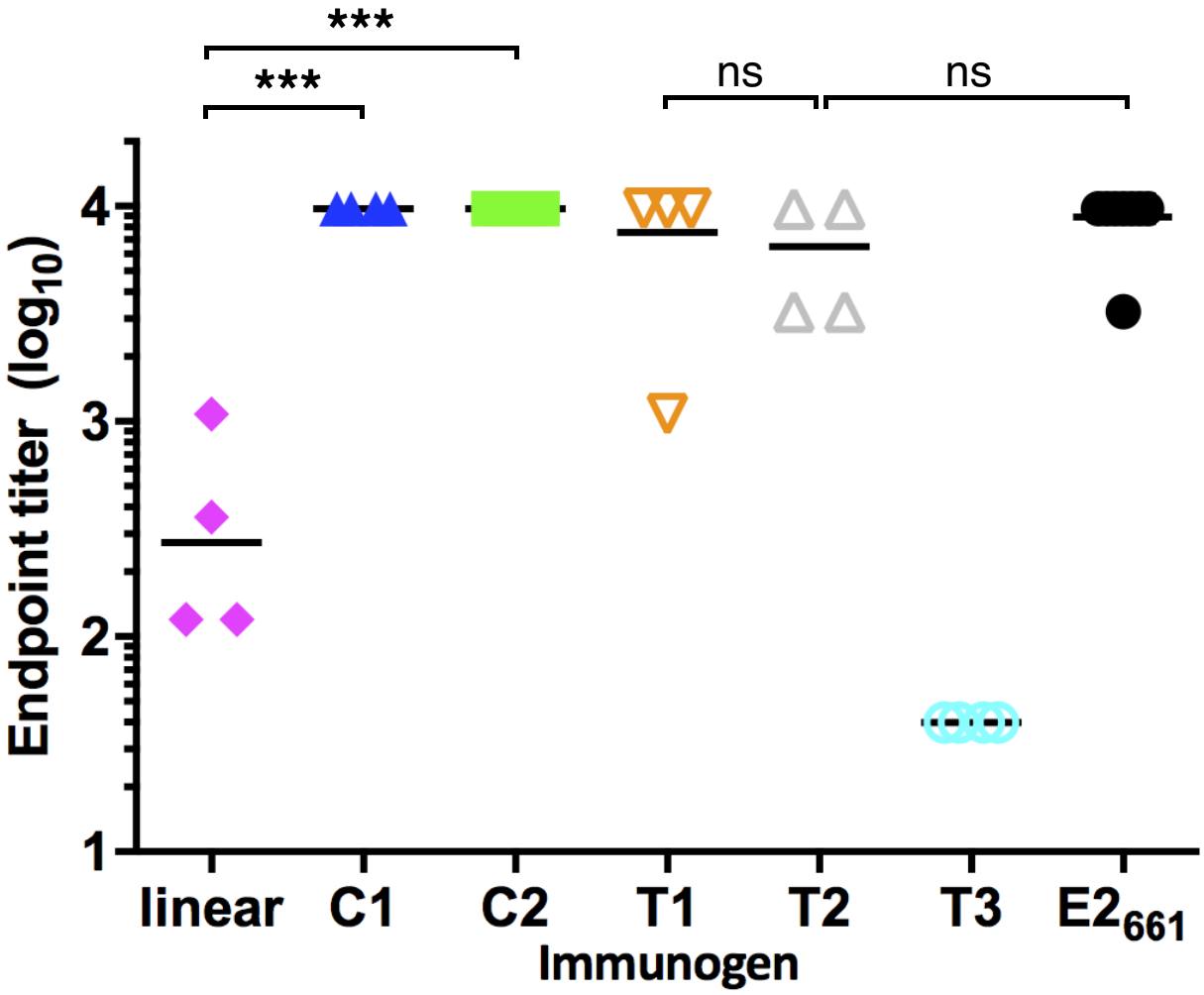

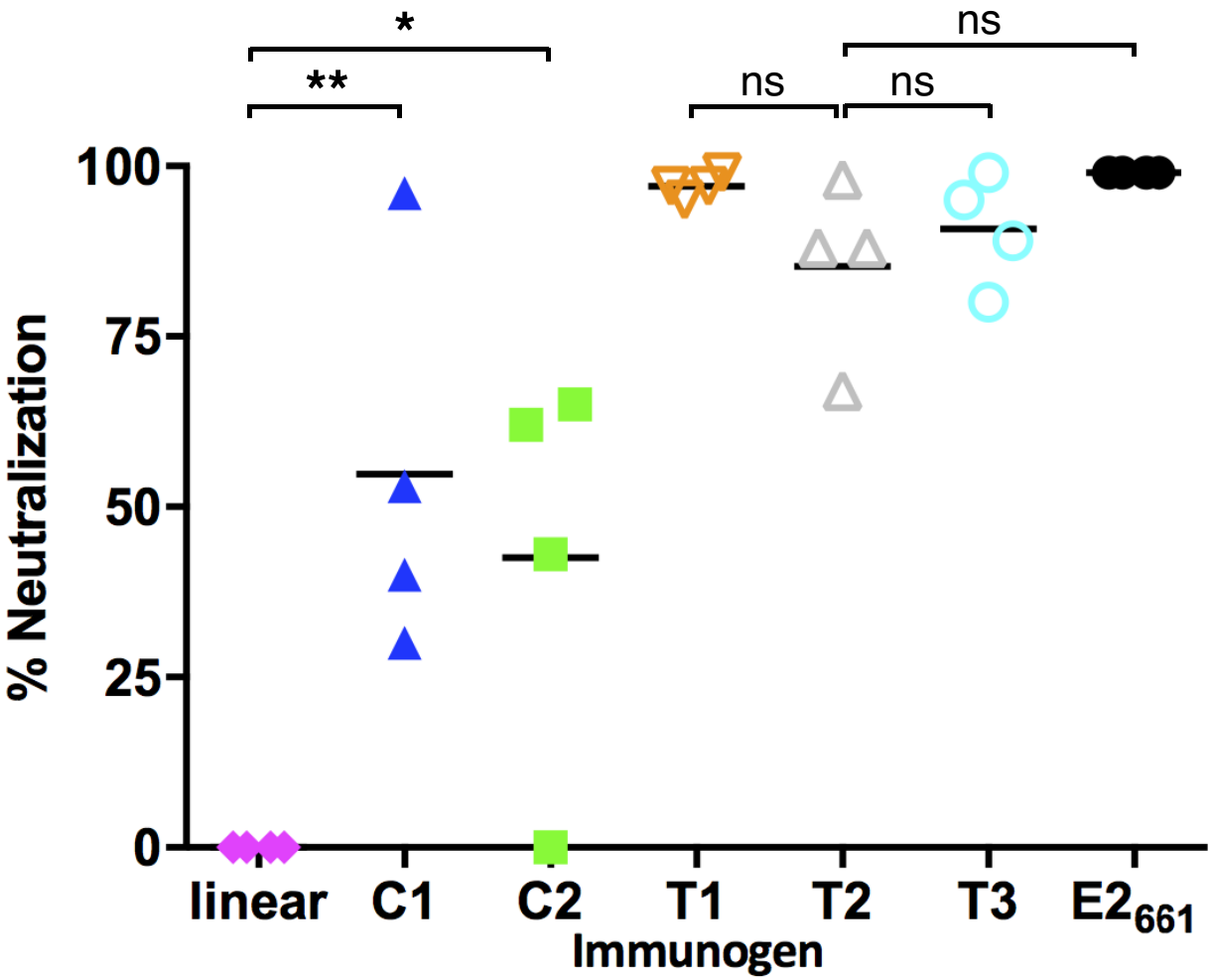

Table 1. X-ray data collection and structure refinement statistics.

	HCV1-C1
Data collection	
Resolution (Å)	29.49–2.26 (2.29–2.26)
Space group	P1
Unit cell	
a, b, c (Å)	47.07, 94.54, 126.76
α, β, γ (°)	91.84, 94.95, 97.91
Reflections	186,455
Unique reflections	96,679 (8,406)
Completeness (%)	92.68 (61.00)
R_{merge} [b]	0.069
Refinement	
R_{work} (%) [a,c]	21.81 (30.99)
R_{free} (%) [a,c]	26.09 (34.27)
No. of protein atoms	14030
No. of water molecules	548
RMSDs from ideality	
Bond length (Å)	0.012
Bond angles (°)	1.59
Ramachandran plot statistics (%)	
Favored	96.1
Allowed	3.6
Forbidden	0.3
PDB Accession Code	5KZP

[a]Values in parentheses are statistics for the highest resolution shell.
[b]Rmerge = $\Sigma_h\Sigma_i I_{hi} - \langle I_h\rangle / \Sigma_{h,i} I_{hi}$ where I_{hi} is the ith observation of the reflection h, while $\langle I_h\rangle$ is its mean intensity.
[c]$R_{work} = \Sigma||F_o| - |F_c||/\Sigma|F_o|$, where F_c is the calculated structure factor. R_{free} is as for R_{work} but calculated for a randomly selected 5% of reflections not included in the refinement.

Table 2. Serum neutralization of immunized mice.

		% Neutralization			
Immunogen	**Mouse #**	**H77 (1a)**	**1b**	**4a**	**H77 ID_{50}**
linear	1	0	-	-	< 64
	2	0	-	-	< 64
	3	0	-	-	< 64
	4	0	-	-	< 64
C1	1	96	0	0	720
	2	40	23	0	< 64
	3	30	0	0	< 64
	4	53	0	0	< 64
C2	1	62	20	4	70
	2	0	0	0	< 64
	3	43	23	0	< 64
	4	65	37	0	110
T1	1	97	64	0	> 5000
	2	99	92	18	> 5000
	3	97	0	0	890
	4	95	91	20	870
T2	1	88	0	18	100
	2	88	15	24	190
	3	98	87	0	> 5000
	4	67	0	8	< 64
T3	1	95	33	16	425
	2	99	27	19	> 5000
	3	80	28	15	75
	4	89	23	45	400
$E2_{661}$	1	99	10	0	> 5000
	2	99	10	23	3470
	3	99	70	0	> 5000
	4	99	10	28	> 5000

Percent neutralization was measured using HCV pseudoparticle (HCVpp) assays and is shown for 1:64 serum dilution, with HCVpp representing genotypes 1a (isolate H77), 1b (isolate 1b-#2), and 4a (isolate 4a-MJ). Dilution levels corresponding to 50% neutralization (ID_{50}) were calculated for H77 by curve fitting in GraphPad Prism software. Highlighted cells denote > 50% neutralization at 1:64 dilution, or H77 $ID_{50} \geq$ 100. Due to low H77 neutralization, genotype 1b and 4a HCVpp neutralization of linear peptide-immunized mice was not tested.